Title:

Isolation and characterization of novel high-CO$_2$ requiring mutants of *Chlamydomonas reinhardtii*

Authors:

Lianyong Wang[1], Takashi Yamano[1], Masataka Kajikawa[1], Masafumi Hirono[2], Hideya Fukuzawa[1]

[1] *Graduate School of Biostudies, Kyoto University, Kyoto, 606-8502, Japan*

[2] *Graduate School of Science, University of Tokyo, Tokyo, 113-0033, Japan*

Corresponding Author:

Hideya Fukuzawa

Graduate School of Biostudies, Kyoto University, Kyoto, 606-8502, Japan

Phone: +81-75-753-6277

FAX: +81-75-753-9228

E-mail: fukuzawa@lif.kyoto-u.ac.jp

1

Abstract

Aquatic microalgae induce a carbon-concentrating mechanism (CCM) to maintain photosynthetic activity in low-CO_2 conditions. Although the molecular mechanism of the CCM has been investigated using the single cell green alga *Chlamydomonas reinhardtii*, and several CCM-related genes have been identified by analyzing high-CO_2 (HC)-requiring mutants, many aspects of the CO_2-signal transduction pathways remain to be elucidated. In this study, we report the isolation of novel HC-requiring mutants defective in the induction of CCM by DNA tagging. Growth rates of 20,000 transformants grown under HC and low-CO_2 conditions were compared, and three HC-requiring mutants (H24, H82, and P103) were isolated. The photosynthetic CO_2-exchange activities of these mutants were significantly decreased compared with that of wild-type cells, and accumulation of HLA3 and both LCIA and HLA3 were absent in mutants H24 and H82, respectively. Although the insertion of the marker gene and the HC-requiring phenotype were linked in the tetrad progeny of H82, and a calcium-sensing receptor CAS was disrupted by the insertion, exogenous expression of CAS alone could not complement the HC-requiring phenotype.

Keywords

Introduction

Some aquatic photosynthetic organisms possess a carbon-concentrating mechanism (CCM) to maintain optimal photosynthetic activity under CO_2-limiting conditions caused by the slow CO_2 diffusion rate in aquatic environments and the low catalytic capacity of ribulose 1, 5-bisphosphate carboxylase-oxygenase (Rubisco) – the CO_2 fixation enzyme. In *Chlamydomonas reinhardtii*, a single cell green alga, the CCM operates by inducing numerous CCM-related proteins involved in acquiring dissolved inorganic carbon (Ci; CO_2 and HCO_3^-) from external sources and generating elevated levels of HCO_3^- in the stroma (Moroney and Ynalvez 2007). In addition to the environmental Ci concentration, induction of the CCM is also dependent on light intensity (Yamano et al. 2008), although it remains unclear whether a change in light intensity has a direct or indirect effect on the induction process.

In order to concentrate HCO_3^- in the chloroplast stroma, a low-CO_2 (LC)-inducible Ci-transport system is needed (Spalding 2008; Wang et al. 2011). Membrane proteins LCI1, LCIA, and HLA3 are considered to associate with Ci transport under LC conditions. LCIA is a member of the Formate/Nitrite Transporter (FNT) family and its transcription level is strongly induced by LC stress (Miura et al. 2004). The expression of LCIA in *Xenopus* oocytes led to uptake activity of NO_2^- as well as HCO_3^- (Mariscal et al. 2006). LCI1 is localized to the plasma membrane, and exogenous expression of LCI1 under high-CO_2 (HC) conditions showed an increased photosynthetic affinity for Ci and intracellular Ci accumulation (Ohnishi et al. 2010). HLA3 belongs to an ATP-binding cassette (ABC) transporter superfamily and is predicted to localize to the plasma membrane (Im and Grossman 2002). A recent study showed that simultaneous knockdown of *HLA3* and *LCIA* caused a dramatic decrease in

growth rate, photosynthetic Ci affinity, and Ci accumulation, indicating that these proteins are cooperatively associated with Ci transport as part of the CCM (Duanmu et al. 2009).

CCM1 (also known as CIA5) has been identified as a regulatory factor for the induction of *LCI1*, *LCIA*, and *HLA3* under LC conditions (Fukuzawa et al. 2001; Xiang et al. 2001; Miura et al. 2004). Moreover, the fact that the induction of almost all LC-inducible genes is impaired in a *ccm1* mutant suggests that CCM1 is a master regulator of the CCM through the LC signal transduction pathway (Miura et al. 2004; Fang et al. 2012). Moreover, downstream of CCM1, the LC-inducible MYB DNA-binding transcriptional regulator LCR1 was identified and shown to function as a transmitter and amplifier of the LC signal from CCM1 to at least three LC-inducible genes, *CAH1*, *LCI1*, and *LCI6* (Yoshioka et al. 2004).

Although the function of CCM1 and LCR1 as key regulators of CCM-related genes has been investigated, the full CO_2-signal transduction pathway remains unclear, possibly because of the small number of regulatory mutants isolated. In this study, we report the isolation of HC-requiring mutants showing retarded growth rates in LC conditions. By examining the photosynthetic characteristics and expression profiles of these CCM-related proteins, the obtained mutants were shown to be defective in Ci transporters.

Materials and methods

Strains and culture conditions

C. reinhardtii strain C9 (photosynthetically wild-type (WT) strain available from the National Institute for Environmental Studies, Japan, as strain NIES-2235) and

CCM1-disrupted mutant C16 (Fukuzawa et al. 1998) were cultured in

Tris-acetate-phosphate (TAP) medium for maintenance. For physiological analyses and

western blot analyses, cells were first photoautotrophically cultured in a modified

high-salt medium (HSM) containing 20 mM MOPS aerated with air enriched with 5%

CO_2 (HC conditions) for 12 h. And then, the cultures were diluted five-times with

modified HSM and divided into two culture tubes aerated with HC or ordinary air

containing 0.04% CO_2 (LC conditions) for 12 h, respectively, at 25°C under continuous

illumination at 80 μmol photons m^{-2} s^{-1}.

Transformation of cells

A 1,999-bp DNA fragment containing the hygromycin (hyg)-resistant gene *aph7''*

driven by β$_2$-tublin promoter was amplified by PCR from plasmid pHyg3 (Berthold et al.

2002) using PrimeSTAR GXL DNA Polymerase (TAKARA BIO, Shiga, Japan) by

35 cycles of denaturation for 10 s at 98°C, annealing for 15 s at 60°C, and extension for

2 min at 68°C with a forward primer

(5'-GCACCCCAGGCTTTACACTTTATGCTTCC-3') and reverse primer

(5'-CCATTCAGGCTGCGCAACTGTTGG-3'). Similarly, a 1,534-bp DNA fragment

containing the paromomycin (par)-resistance gene *aph8''* driven by *HSP70A* (heat

shock protein 70 A)-*RBCS2* tandem promoter (Lodha et al. 2008), was amplified by

PCR from plasmid pGenD-aphVIII (Nakazawa et al. 2007) using PrimeSTAR GXL

DNA Polymerase by 30 cycles of denaturation for 10 s at 98°C, annealing for 15 s at

60°C, and extension for 2 min at 68°C with a forward primer

5'-GCTTATCGATACCGTCGACCT-3' and reverse primer

5'-AACACCATCAGGTCCCTCAG-3'. The PCR product was purified using a PCR

purification kit (QIAGEN, Valencia, CA, USA) and the concentration was adjusted to 100 µg mL^{-1}.

Transformation of *C. reinhardtii* cells without cell-wall degradation was performed as reported previously (Yamano et al. 2013). Briefly, C9 cells in early logarithmic phase were collected and transformed by electroporation using a NEPA21 electroporator (NEPAGENE, Chiba, Japan). The transformants were incubated at 25°C for 24 h with gentle agitation under illumination at 1.5 µmol photons m^{-2} s^{-1} and then screened on TAP plates containing 30 µg mL^{-1} hyg or 10 µg mL^{-1} par at 25°C under 80 µmol photons m^{-2} s^{-1}. After 4 days, colonies of transformants appeared and then subjected to the screening process of HC-requiring mutants.

Screening of high-CO$_2$-requiring mutants

Cells grown under HC conditions for 12 h were replicated into two 96-well microtiter plates containing liquid HSM medium. One of the plates was incubated in a chamber supplied with LC air and the other in the chamber supplied by HC air for 3 days. Every 24 h, optical density at 700 nm (OD$_{700}$) was measured using a microtiter plate reader XFluor4 (TECAN, Tokyo, Japan). For the first screening, transformants whose OD$_{700}$ under HC conditions did not reached to 1.0 at 72 h were discarded, and transformants whose OD$_{700}$ under LC conditions was less than five-times of the initial OD$_{700}$ were selected as candidate HC-requiring mutants. For the second screening, the candidate mutants grown in liquid HSM medium under HC conditions were diluted to OD$_{430}$ of 0.15, 0.07, or 0.03, and 3 µL of each cell suspension was spotted onto two solid HSM agar plates, and grown in HC or LC chambers for 9 days.

Measurement of light-dependent CO₂-exchange activity and inorganic

carbon-dependent photosynthetic oxygen evolution

For measuring light-dependent CO_2-exchange (LCE) activity, harvested cells after

growth in HC or LC conditions were suspended in fresh HSM medium at 5 μg Chl mL^{-1}.

LCE activity of the cell suspension was measured using an open infrared gas analysis

system with 50 ppm CO_2, as described previously (Yamano et al. 2008).

The affinity for Ci was evaluated by measuring the rate of dissolved

Ci-dependent photosynthetic oxygen (O_2) evolution. Cells were collected by

centrifugation and then resuspended in Ci-depleted 50 mM HEPES-NaOH buffer (pH

7.8) at 15 μg mL^{-1} chlorophyll. Photosynthetic O_2 was measured using a Clark-type O_2

electrode (Hansatech Instruments, Norfolk, UK) as described previously (Yamano et al.

2008). The maximum O_2-evolving activity, defined as V_{max}, was measured in the

presence of 10 mM NaHCO₃.

Immunoblotting analysis

Extracted soluble proteins and membrane proteins suspended in sodium dodecylsulfate

(SDS) gel-loading buffer containing 50 mM Tris-HCl (pH 8.0), 25% glycerol (w/v), 2%

SDS, and 0.1 M DTT were incubated at 65°C for 10 min or 100°C for 1 min and

subsequently centrifuged at 14,000 g for 3 min. The supernatant containing solubilized

proteins was subjected to SDS-PAGE analysis. After electrophoresis, proteins were

electrophoretically transferred to polyvinylidene difluoride membranes (Bio-Rad,

Hercules, CA, USA). Membranes were blocked with 5% (w/v) non-fat skim milk

(Wako, Osaka, Japan) in phosphate-buffered saline (PBS). Blocked membranes were

washed with PBS containing 0.1% (v/v) Tween-20 (PBS-T) and treated with the

following antibodies in PBS-T: anti-CCM1 antibody (1:5,000 dilution); anti-CAH1

antibody (1:2,500 dilution); anti-CAH3 antibody (1:2,000 dilution); anti-CAH6

antibody (1:2,000 dilution); anti-LCI1 antibody (1:5,000 dilution); anti-HLA3 antibody

(1:1,000 dilution); anti-LCIA antibody (1:5,000 dilution); anti-LCIB antibody (1:5,000

dilution); anti-LCIC antibody (1:10,000 dilution); and anti-Histone H3 antibody

(1:10,000 dilution). A horseradish peroxidase-conjugated goat anti-rabbit IgG antibody

(1:10,000 dilution; GE Healthcare, Milwaukee, WI, USA) was used as a secondary

antibody. Immunologically positive signals were visualized using Luminata Crescendo

Western HPR substrate (Millipore, Billerica, MA, USA) and detected using an

ImageQuant LAS 4000 (Fuji Film, Tokyo, Japan).

Thermal asymmetric interlaced PCR

For the thermal asymmetric interlaced (TAIL) PCR analysis of upstream flanking

regions, specific primers UP-3 (5'-GACTCACCTCCCAGAATTCCTGG-3'), UP-2

(5'-TCGTTCCGCAGGCTCGCGTAGG-3'), and UP-1

(5'-TCGAGAAGTAACAGGGATTCTTGTGTCATG-3') were used for primary,

secondary, and tertiary reactions, respectively. Similarly, for downstream flanking

regions, DP-4 (5'-CTTCGAGGTGTTCGAGGAGACCC-3'), DP-3

(5'-CGCTGGATCTCTCCGGCTTCACC-3'), and DP-2

(5'-GCCCCCGGCGCCTGATAAGG-3') were used for primary, secondary, and tertiary

reactions, respectively. We also used the degenerate primers RMD227 (Dent et al. 2005),

A1 (5'-NGTCGASWGANAWGAA-3'), A3 (5'-WGTGNAGWANCANAGA-3'), A4

(5'-TGWGNAGSANCASAGA-3'), and A7 (5'-NTCGASTWTSGWGTT-3') (Liu et al.

1995; Liu and Whittier 1995). The genomic DNA was diluted 10-fold, and 1 μL aliquots

were used. Primary reactions with 1× GC buffer (TAKARA BIO), 0.2 mM dNTPs, 5 pmol of specific primer, 60 pmol of degenerate primer, and 1 U of LA Taq (TAKARA BIO) were performed under the following conditions: 2 min, 95°C; 5 cycles (1 min, 94°C; 1 min, 62°C; 2.5 min, 68°C); 1 min, 94°C; 3 min, 25°C; ramping over 3 min to 68°C; 2.5 min, 68°C; 15 cycles (30 s, 94°C; 3.5 min, 68°C; 30 s, 94°C; 3.5 min, 68°C; 30 s, 94°C; 1 min, 44°C; 2.5 min, 68°C); 5 min, 68°C. The primary reaction products were diluted 50-fold, and 1 μL aliquots were subjected to secondary reactions with identical components to the primary reaction under the following conditions: 12 cycles (30 s, 94°C; 3.5 min, 68°C; 30 s, 94°C; 3.5 min, 68°C; 30 s, 94°C; 1 min, 44°C; 2.5 min, 68°C); 5 min, 68°C. The secondary reaction products were diluted 50-fold, and 1 μL aliquots were subjected to tertiary reactions with identical components to the primary reaction under identical conditions to the secondary reaction. The tertiary reaction products were separated by agarose gel electrophoresis, fragments were extracted from the gel, and their sequences were analyzed.

For genomic PCR of flanking regions of hyg cassette and sequencing of the upstream and downstream PCR products, primers of F1 (5'-GCGGATCAGATAATACCCCGTA-3'), R1 (5'-AAGAACAGGGGGCTGAGGTAAT-3'), R2 (5'-AGACTGTGAAGCCATGCCCAGGTAGC-3'), UP-S (5'-TCATGTTTGCGGGTTGTGACTG-3'), and DP-S (5'-CCCCGCTCCGTGTAAATGGAGG-3') were used and their locations were depicted in Fig. 4B.

Quantitative real-time PCR

RNA was extracted from cells grown under HC or LC conditions using an RNeasy Plant Mini Kit (QIAGEN) and any remaining genomic DNA was digested with DNase (QIAGEN) in accordance with the manufacturer's instructions. First strand complementary DNA was synthesized using Superscript III Reverse Transcriptase (Life Technology, Carlsbad, CA, USA). Quantitative real-time PCR was performed using SYBR Premix Ex Taq GC (TAKARA BIO) and a LightCycler 480 Instrument (Roche, Mannheim, Germany) in accordance with the manufacturer's instructions. *CBLP* encoding a receptor of activated protein kinase C was used as an internal control. The primers used were *CAS* (5'-CCTCAGCCCCTGTTCTTCG-3' and 5'-CGCGGATGTCGATCAGCAC-3'), *HLA3* (5'-CGCTCTGCGCAAGTCCTTC-3' and 5'-CGTAGTTGACGTGGGACAGCA-3'), *LCIA* (5'-TCTCCGTGGGAGGCAACATC-3' and 5'-ACAGACCCACGGGGAACACC-3'), *CBLP* (5'-AGGTCTGGAACCTGACCAACT-3' and 5'-AAGCACAGGCAGTGGATGA-3'). The amplification conditions were as follows: 5 min denaturation at 95°C; 40 cycles at 95°C for 10 s, at 55°C for 30 s and at 68°C for 1 min. Melting curves for each PCR product were determined by measuring the decrease in fluorescence with increasing temperature from 60°C to 95°C.

Expression of hemagglutinin epitope-tagged CAS

For constructing the expression plasmid of hemagglutinin (HA) epitope-tagged CAS, genomic region of *CAS* was amplified by PCR with forward primer (5'-CACAACAAGCCCATATGCAGCTTGCTAACGCTCCTCGCCTCGCGGCC-3') and reverse primer (5'-GGTATCGATCGAATTCCGAGCGGGGGGCGGGCAGGCGGCGGGTCGA-3').

The PCR product was cloned into the *Nde*I and *Eco*RI sites of the expression vector pGenD-HA (Nakazawa et al. 2007) using the In-Fusion reaction (Clontech, Mountain View, CA, USA). The resulting fusion protein contained a HA sequence at its C-terminus. HA-tagged CAS was detected by Anti-HA-Peroxidase, High Affinity 3F10 (1:5,000 dilution; Roche).

Tetrad analysis

The tetrad analysis was performed using an inverted microscope (BX41; Olympus, Tokyo, Japan) equipped with a micromanipulator (Narishige, Tokyo, Japan) and a glass needle (Singer Instruments, Somerset, UK) as described previously (Nishimura et al. 2012).

Results

Isolation of high-CO_2-requiring mutants

In screening, HC-requiring mutants were obtained by comparing the growth rates of cells between HC and LC conditions (Fig. 1A). First, to construct insertion mutant libraries, WT strain C9 was transformed with hyg or par resistance cassettes. In total, approximately 20,000 transformants (10,000 for hyg and 10,000 for par resistance) were generated. For the first screening, the OD_{700} of each transformant grown under HC or LC conditions was compared, and 655 transformants showing retarded growth rates under LC conditions were selected as candidate HC-requiring mutants. For the second screening, these candidates were spotted on HSM agar plates and tested for their growth ability under HC or LC conditions, and transformants showing retarded or no growth under LC conditions were selected. As a result, three mutants, designated as H24, H82,

and P103, were isolated as HC-requiring mutants (Fig. 1B). Although the WT cells could grow well under LC conditions as well as HC conditions, the mutants showed little growth under LC conditions.

Photosynthetic characteristics of the mutants

To evaluate the photosynthetic characteristics of the obtained mutants, the light-dependent CO_2-exchange (LCE) activities were measured (Table 1). As a control of HC-requiring mutant, strain C16 deficient in CCM1 was used. Under LC conditions, C16, H24, H82, and P103 showed drastically decreased LCE activities of 19.7 (16.3%), 10.9 (9.1%), 13.5 (11.2%), and 19.7 (16.4%) µmol CO_2 mgChl^{-1} h^{-1}, respectively, compared with 120.2 µmol CO_2 mgChl^{-1} h^{-1} for WT cells (Table 1), suggesting lower Ci uptake activity under LC conditions.

Next, the rates of photosynthetic O_2 evolution under changing external Ci concentrations were measured (Fig. 2 and Table 1). Under LC conditions, C16, H82, and P103 showed much higher photosynthetic $K_{0.5}$ (Ci) values of 482.0, 525.6, and 312.4 µM, respectively, compared with a WT value of 48.8 µM, indicating that photosynthetic affinity for Ci was drastically decreased in the mutants. In contrast, LC-acclimated H24 showed typical photosynthetic responses of cells expressing the CCM in the range of 10 to 100 µM Ci and showed approximately 70% of maximal photosynthetic rate at 100 µM Ci. Although the photosynthetic rate of WT cells reached a maximum at 100 µM Ci and retained its activity, the photosynthetic rate of H24 did not increase and attenuated between 100 and 500 µM Ci. The rates then increased again at higher concentrations of Ci, reaching a maximum at 1.5 mM Ci. Although this biphasic response of the photosynthetic curve caused an apparent decrease in the $K_{0.5}$

(Ci) value of 50.4 μM, attenuated photosynthetic activity between 100 μM and 500 μM, which corresponds to LC conditions, could cause the retarded growth of H24.

Accumulation of carbon concentrating mechanism-related proteins

It was speculated that the absence of some CCM-related proteins led to the HC-requiring phenotype of the mutants. To examine the accumulation of CCM-related proteins, soluble or membrane proteins were extracted from WT, C16, H24, H82, and P103 cells grown under HC or LC conditions. These protein samples were probed with antibodies against CCM-related proteins, including CCM1, CAH1, CAH3, CAH6, LCI1, HLA3, LCIA, LCIB, and LCIC (Fig. 3).

In the P103 mutant, CCM1 was not detected, and the accumulation profiles of CCM-related proteins were quite similar to that of C16, suggesting that P103 could be a *CCM1* mutant. By sequencing the genomic region of *CCM1* in P103, a deletion of adenine in the second exon was found (AAAAA in WT and AAAA in P103), causing a frame shift, producing truncated CCM1 with 161 amino acid residues.

In the WT cells, CCM1, CAH3, and CAH6 were accumulated constitutively irrespective of the environmental CO_2 conditions. Although CCM1 and CAH6 accumulated normally in H24 and H82 cells, a slight decrease in CAH3 was observed in C16, H24, H82, and P103 cells. Accumulation profiles of LCIB and LCIC in H24 and H82 cells were similar to that of WT cells with slight accumulation under HC conditions and induced accumulation under LC conditions, as reported previously. HLA3 and LCIA are LC-inducible membrane proteins associated with Ci transport. In LC-acclimated H24 and H82 cells, accumulation of HLA3 or both HLA3 and LCIA, respectively, were not detected.

Genetic linkage between the high-CO$_2$-requiring phenotype and insertion site of a hygromycin resistance cassette in H82 mutant cells

In order to evaluate a genetic link between the HC-requiring phenotype and insertion of the hyg resistance cassette, H82 cells were crossed with WT strain CC-1690 or CC-125. In total, 96 progenies generated from 24 complete tetrads (A-L from H82×CC-1690 in Supplementary Fig. S1 and M-X from H82×CC-125 in Supplementary Fig. S2) were obtained, and the linkage between the HC-requiring phenotype and hyg resistance was analyzed (Fig. 4A). All progenies showing the HC-requiring phenotype possessed a hyg insertion detected by PCR, suggesting that the mutation in H82 appeared to be caused by a single insertion event.

To determine the flanking region of the hyg cassette, TAIL-PCR was performed. Using UP and DP primers located in the promoter region and 3'-untranslated region (UTR) of the hyg cassette, respectively, both sides of the insertion were sequenced. Comparison of the obtained nucleotide sequence with the *C. reinhardtii* genomic sequence database Phytozome v.9.1 yielded a match to locus *Cre12.g497300* encoding CAS, a calcium-sensing receptor (Fig. 4B). Specifically, the obtained sequence from the UP side matched with a sequence in the 4th intron and that from the DP side matched with a sequence in the 5th exon, correlating with a deletion of 92-bp in *CAS*. The F1/R1 primer set, homologous to the 4th intron and 5th exon, amplified PCR products of 365-bp from WT and of approximately 7-kb from H82, confirming the hyg insertion in *CAS*. Considering that the length of the hyg cassette was 1,999-bp, three or four copies of the cassette could be tandemly inserted. Hyg insertion was also confirmed by PCR using several primer sets of F1/UP-S (Fig 4C), DP-S/R1

(Supplementary Fig. S1), and DP-S/R2 (Supplementary Fig. S2).

To investigate whether exogenous expression of *CAS* could complement the HC-requiring phenotype of H82, two independent lines expressing HA-tagged CAS (#10 and #13) were isolated (Fig. 4D). In these strains, however, LC-inducible accumulation of LCIA and HLA3 were not complemented. Quantitative real-time PCR also confirmed that LC-inducible expression of *LCIA* and *HLA3* was not complemented in spite of a significant level of accumulation of exogenous HA-tagged CAS protein.

Discussion

Rapid construction of insertion mutant libraries using a square pulse electroporator

This study showed the isolation of novel HC-requiring mutants defective in induction of the CCM. Although several studies have reported the screening of *C. reinhardtii* mutants by DNA tagging (Prieto et al. 1996; Fukuzawa et al. 1998; Dent et al. 2005), making insertion mutant libraries has been a time-consuming process. In this study, we firstly used a square electric pulse-generating electroporator for constructing of the libraries. Because of its high efficiency of transformation and speed from preparing cells without removing the cell wall (Yamano et al. 2013), constructing libraries could became a non-limiting step for mutants screening studies.

Relationship between the absence of inorganic carbon transporters and high-CO$_2$-requiring phenotype

The slow growth rates and decreased LCE activity of the obtained mutants under LC conditions indicated that supplying HC is essential for survival (Fig. 1B). Among the CCM-related proteins examined, only HLA3 was missing in H24. It was reported that

knockdown of *HLA3* alone resulted in only modest decreases in photosynthetic Ci

affinity and Ci uptake at neutral pH conditions (Duanmu et al. 2009). In spite of this

result, H24 cells could not grow under LC condition, as shown in spot tests performed

at pH 7.0. This was possibly because the completely absence of HLA3 accumulation in

H24 mutant caused a more severe phenotype than achieved with knockdown of *HLA3*.

Alternatively, we cannot rule out the possibility that the absence of HLA3 was not the

main cause of the HC-requiring phenotype, and the accumulation of other proteins

related with CCM or photorespiration could be missed. In the H82 mutant, LCIA as

well as HLA3 was not accumulated under LC conditions (Fig. 3). Considering that

simultaneous knockdown of *HLA3* and *LCIA* resulted in dramatic decreases in growth,

Ci uptake, and photosynthetic Ci affinity (Duanmu et al. 2009), the HC-requiring

phenotype of H82 could be mainly caused by the absence of LCIA and HLA3. *LCIA,*

HLA3, and *CAS* are located on chromosome 6, 2, and 12, respectively, and the

HC-requiring phenotype of H82 mutant was closely linked with the hyg cassette insertion

into *CAS* gene on chromosome 12 (Supplementary Fig. S1 and S2). From those results, it

is probable that *LCIA* and *HLA3* themselves were not structurally disrupted in the H82

mutant, although experimental validation is required. Because the transcription of *LCIA*

and *HLA3* was also suppressed in H82 (Fig. 4E), the genes responsible for H82 could be

a transmitter of the LC signal from CCM1 to at least *LCIA* and *HLA3*, which would be

analogous to the function of LCR1 for the regulation of LCI1 (Yoshioka et al. 2004).

To identify the gene responsible for the phenotype of H82, its tetrad progenies

were characterized, and it was shown that the *CAS* gene was disrupted by the insertion

of hyg cassette. In a previous knockdown analysis of the *CAS* gene, CAS was shown to

be involved in the acclimation to the high-light (HL) stress particularly by regulating

LHCSR3 expression (Petroutsos et al. 2011) and the Ca^{2+}-dependent regulation of cyclic

photosynthetic electron flow of photosynthesis (Terashima et al. 2012). Considering the

fact that cyclic photosynthetic electron flow activity was increased under LC conditions

(Lucker and Kramer 2013), the expression of *LHCSR3* was regulated by LC as well as

HL (Yamano et al. 2008), and the HL has a effect on induction of the CCM as LC

conditions (Yamano et al. 2008), it is reasonable to say that CAS could be associated

with the cross-talk between HL and LC stress. Unfortunately, HA-tagged CAS

introduced into H82 could not complement the HC-requiring phenotype as well as the

expression of *HLA3* and *LCIA* under LC conditions (Fig. 4E). Based on these results, it

is possible that the HC-requiring phenotype and suppression of *LCIA* and *HLA3* under

LC conditions was not attributed to the disruption of CAS alone. However, we could not

exclude the possibilities that exogenously expressed HA-tagged CAS could not function

in vivo because of the addition of HA-tag to the C-terminal end of CAS and that the

disruption of other gene along with *CAS* could be attributed to the phenotype of H82. As

far as tetrad progenies tested were concerned, hyg insertion into *CAS* determined by

PCR was closely linked with the HC-requiring phenotype of H82 (Supplementary Fig.

S1 and S2), suggesting that the genetic locus responsible for the HC-requiring

phenotype could be located near to *CAS*. Considering the case of point mutation of

CCM1 in the P103 mutant, we cannot rule out the possibilities that there could be point

mutations, large-scale deletions, rearrangements, or insertion of small portion of hyg

cassette which could not detected by TAIL-PCR or Southern blot analysis in the

responsible gene of H82 mutant.

   For identifying the responsible genes of mutants, complementation assay

using genomic libraries constructed from bacterial artificial chromosome clones is

17

useful approach (von Gromoff et al. 2008). Additionally, massive data generated by whole genome sequencing succeeded in the determination of point mutation sites of the *Chlamydomonas* flagella mutants (Lin et al. 2013). Further analyses including these techniques would reveal the disrupted gene responsible for the HC-requiring phenotype of H82 mutant and whether the actual mutation causes the absence of LCIA and HLA3 or not.

References

Berthold P, Schmitt R, Mages W (2002) An engineered *Streptomyces hygroscopicus aph 7″* gene mediates dominant resistance against hygromycin B in *Chlamydomonas reinhardtii*. Protist 153:401–412

Dent RM, Haglund CM, Chin BL, Kobayashi MC, Niyogi KK (2005) Functional genomics of eukaryotic photosynthesis using insertional mutagenesis of *Chlamydomonas reinhardtii*. Plant Physiol 137:545–556

Duanmu D, Miller AR, Horken KM, Weeks DP, Spalding MH (2009) Knockdown of limiting-CO_2-induced gene *HLA3* decreases HCO_3^- transport and photosynthetic Ci affinity in *Chlamydomonas reinhardtii*. Proc Natl Acad Sci USA 106:5990–5995

von Gromoff ED, Alawady A, Meinecke L, Grimm B, Beck CF (2008) Heme, a plastid-derived regulator of nuclear gene expression in *Chlamydomonas*. Plant Cell 20:552–567

Fang W, Si Y, Douglass S, Casero D, Merchant SS, Pellegrini M, Ladunga I, Liu P, Spalding MH (2012) Transcriptome-wide changes in *Chlamydomonas reinhardtii* gene expression regulated by carbon dioxide and the CO_2-concentrating mechanism regulator CIA5/CCM1. Plant Cell 24:1876–1893

Fukuzawa H, Ishizaki K, Miura K, Matsueda S, Matsueda S, Ino-ue T, Kucho K, Ohyama K (1998) Isolation and characterization of high-CO_2 requiring mutants from *Chlamydomonas reinhardtii* by gene tagging. Can J Bot 76:1092–1097

Fukuzawa H, Miura K, Ishizaki K, Kucho KI, Saito T, Kohinata T, Ohyama K (2001) *Ccm1*, a regulatory gene controlling the induction of a carbon-concentrating mechanism in *Chlamydomonas reinhardtii* by sensing CO_2 availability. Proc Natl Acad Sci USA 98:5347–5352

Im CS, Grossman AR (2002) Identification and regulation of high light-induced genes in *Chlamydomonas reinhardtii*. Plant J 30:301–313

Lin H, Nauman NP, Albee AJ, Hsu S, Dutcher SK (2013) New mutations in flagellar motors identified by whole genome sequencing in *Chlamydomonas*. Cilia 2:14

Liu YG, Mitsukawa N, Oosumi T, Whittier RF (1995) Efficient isolation and mapping of *Arabidopsis thaliana* T-DNA insert junctions by thermal asymmetric interlaced PCR. Plant J 8:457–463

Liu YG, Whittier RF (1995) Thermal asymmetric interlaced PCR: Automatable amplification and sequencing of insert end fragments from P1 and YAC clones for chromosome walking. Genomics 25:674–681

Lodha M, Schulz-Raffelt M, Schroda M (2008) A new assay for promoter analysis in *Chlamydomonas* reveals roles for heat shock elements and the TATA box in *HSP70A* promoter-mediated activation of transgene expression. Eukaryot Cell 7:172–176

Lucker B, Kramer DM (2013) Regulation of cyclic electron flow in *Chlamydomonas reinhardtii* under fluctuating carbon availability. Photosynth Res 117:449–459

Mariscal V, Moulin P, Orsel M, Miller AJ, Fernández E, Galván A (2006) Differential regulation of the *Chlamydomonas Nar1* gene family by carbon and nitrogen. Protist 157:421–433

Miura K, Yamano T, Yoshioka S, Kohinata T, Inoue Y, Taniguchi F, Asamizu E, Nakamura Y, Tabata S, Yamato KT, Ohyama K, Fukuzawa H (2004) Expression profiling-based identification of CO_2-responsive genes regulated by CCM1 controlling a carbon-concentrating mechanism in *Chlamydomonas*. Plant Physiol 135:1595–1607

Moroney JV, Ynalvez R (2007) Proposed carbon dioxide concentrating mechanism in

Chlamydomonas reinhardtii. Eukaryot Cell 6:1251–1259

Nakazawa Y, Hiraki M, Kamiya R, Hirono M (2007) SAS-6 is a cartwheel protein that establishes the 9-fold symmetry of the centriole. Curr Biol 17:2169-2174

Nishimura Y, Shikanai T, Nakamura S, Kawai-Yamada M, Uchimiya H (2012) Gsp1 triggers the sexual developmental program including inheritance of chloroplast DNA and mitochondrial DNA in *Chlamydomonas reinhardtii*. Plant Cell 24:2401–2414

Ohnishi N, Mukherjee B, Tsujikawa T, Yanase M, Nakano H, Moroney JV, Fukuzawa H (2010) Expression of a low CO_2-inducible protein, LCI1, increases inorganic carbon uptake in the green alga *Chlamydomonas reinhardtii*. Plant Cell 22:3105–3117

Petroutsos D, Busch A, Janssen I, Trompelt K, Bergner SV, Weinl S, Holtkamp M, Karst U, Kudla J, Hippler M (2011) The chloroplast calcium sensor CAS is required for photoacclimation in *Chlamydomonas reinhardtii*. Plant Cell 23:2950–2963

Prieto R, Pardo JM, Niu X, Bressan RA, Hasegawa PM (1996) Salt-sensitive mutants of *Chlamydomonas reinhardtii* isolated after insertional tagging. Plant Physiol 112:99–104

Spalding M (2008) Microalgal carbon-dioxide-concentrating mechanisms: *Chlamydomonas* inorganic carbon transporters. J Exp Bot 59:1463–1473

Terashima M, Petroutsos D, Hüdig M, Tolstygina I, Trompelt K, Gäbelein P, Fufezan C, Kudla J, Weinl S, Finazzi G, Hippler M (2012) Calcium-dependent regulation of cyclic photosynthetic electron transfer by a CAS, ANR1, and PGRL1 complex. Proc Natl Acad Sci USA 109:17717–17722

Wang Y, Duanmu D, Spalding MH (2011) Carbon dioxide concentrating mechanism in *Chlamydomonas reinhardtii*: inorganic carbon transport and CO_2 recapture. Photosynth Res 109:115–122

Xiang Y, Zhang J, Weeks DP (2001) The *Cia5* gene controls formation of the carbon

concentrating mechanism in *Chlamydomonas reinhardtii*. Proc Natl Acad Sci USA

98:5341–5346

Yamano T, Miura K, Fukuzawa H (2008) Expression analysis of genes associated with

the induction of the carbon-concentrating mechanism in *Chlamydomonas reinhardtii*.

Plant Physiol 147:340–354

Yamano T, Iguchi H, Fukuzawa H (2013) Rapid transformation of *Chlamydomonas*

reinhardtii without cell-wall removal. J Biosci Bioeng 115:691–694

Yoshioka S, Taniguchi F, Miura K, Inoue T, Yamano T, Fukuzawa H (2004) The novel

Myb transcription factor LCR1 regulates the CO_2-responsive gene *Cah1*, encoding a

periplasmic carbonic anhydrase in *Chlamydomonas reinhardtii*. Plant Cell

16:1466–1477

Figure legends

Fig. 1 Screening of high-CO_2 (HC)-requiring mutants. (A) Schematic illustration of screening process. PCR-amplified hygromycin (hyg) or paromomycin (par) resistance cassettes were introduced into wild-type (WT) cells by electroporation. Colonies of transformants were picked up, cultured in 96-well microtiter plates under HC conditions, and replicated into two plates. One replicate plate each was incubated under HC or low-CO_2 (LC) conditions, and candidate HC-requiring mutants were screened by measuring optical density (1st screening). Reproducibility of the HC-requiring phenotype was checked by a spot test experiment (2nd screening). (B) Spot test of WT and HC-requiring mutants H24, H82, and P103. Cells grown to logarithmic phase were diluted to the indicated optical density (OD_{430} 0.15, 0.07, or 0.03), 3 µL of the cell suspensions were spotted on HSM plates and incubated for 9 days in growth chambers supplied with HC or LC under continuous light at 120 µmol photons m^{-2} s^{-1}. H24 and H82 were hyg resistant and P103 was par resistant.

Fig. 2 Oxygen-evolving activity of wild-type (WT) and transformants in response to external dissolved Ci concentrations. WT and mutants were grown in high-CO_2 (HC; closed circles) or low-CO_2 (LC; open circles) conditions. Photosynthetic oxygen evolution was measured using a Clark-type oxygen electrode in the presence of various concentrations of $NaHCO_3$. Insets show plots at external dissolved Ci concentrations below 500 µM.

Fig. 3 Accumulation of CCM-related proteins. Accumulation of CCM-related proteins in wild-type (WT), C16, H24, H82, and P103 cells was analyzed by protein

immunoblotting analysis. Cells were first grown under high-CO_2 (HC) condition for 12 h and shifted to HC or low-CO_2 (LC) conditions for 12 h. Histone H3 was used as a loading control. Asterisks indicate the non-specific protein bands.

Fig. 4 Molecular characterization of the H82 mutant. (A) Genetic linkage of the hygromycin (hyg) insertion and high-CO_2 (HC)-requiring phenotype. Genomic DNA was extracted from tetrad progeny (A1-A4) from crosses of H82 and CC-1690. Genomic PCR was performed with the primer sets depicted in (B). For spot test, progenies grown to logarithmic phase were diluted to the indicated optical density (OD_{430} 0.15, 0.07, or 0.03), 3 μL of each suspension was spotted onto HSM plates, and incubated in a growth chamber supplied with low-CO_2 (LC). Genetic linkage of each tetrad progeny is shown in Online Resource 1. (B) Schematic representation of the hyg cassette insertion into the genome of the H82 mutant. The untranslated region, exon and hyg cassette are shown as white, black, and gray boxes, respectively. Binding sites of PCR primers are indicated by arrows (not drawn to scale). (C) Confirmation of hyg insertion by genomic PCR. Genomic DNA was extracted from wild-type (WT) and H82 cells, and genomic PCR was performed using the primer sets depicted in (B). M indicates the DNA size marker. (D) Accumulation of HA-tagged CAS (CAS-HA), LCIA, and HLA3 in the WT, H82, and CAS-HA-expressing strains #10 and #13. Asterisk indicates a non-specific protein band. (E) Quantitative real-time PCR of *CAS*, *LCIA*, and *HLA3* in WT, H82, and CAS-HA-expressing strains #10 and #13. The expression levels of *CAS*, *LCIA*, and *HLA3* are shown as white, black, and gray bars, respectively.

Supplementary Fig S1. Genetic linkage analysis of the hygromycin (hyg) insertion and high-CO_2 (HC)-requiring phenotype. Genomic DNA was extracted from tetrad progeny (A-L) from crosses of H82 and CC-1690. Genomic PCR was performed with the primer sets (F1 and UP-S or R1 and DP-S) depicted in Fig. 4B. For spot test, progenies grown to logarithmic phase were diluted to the indicated optical density (OD_{430} 0.15, 0.07, or 0.03), 3 μL of each suspension was spotted onto HSM plates, and incubated in a growth chamber supplied with LC for 4 days.

Supplementary Fig S2. Genetic linkage analysis of the hygromycin (hyg) insertion and high-CO_2 (HC)-requiring phenotype. Genomic DNA was extracted from tetrad progeny (M-X) from crosses of H82 and CC-125. Genomic PCR was performed with the primer set (DP-S and R2) depicted in Fig. 4B. For spot test, progenies grown to logarithmic phase were diluted to the OD_{430} of 0.07, 3 μL of each suspension was spotted onto HSM plates, and incubated in a growth chamber supplied with HC or LC for 6 days. For hyg resistance test, progenies were directly streaked onto TAP plates containing 30 μg mL^{-1} hyg, and incubated under HC condition for 6 days.

Table 1 Photosynthetic parameters of wild-type (WT) and mutants cells

Strain name	CO_2 conditions	CO_2-exchange activity [μmol CO_2 mgCh^{-1} h^{-1}]	V_{max} of O_2-evolving activity [μmol O_2 mgChl^{-1} h^{-1}]	$K_{0.5}$ (Ci) [μM]
WT	HC	28.8 ± 10.8	184.7 ± 13.2	298.7 ± 43.3
	LC	120.2 ± 6.1	197.7 ± 18.7	47.8 ± 5.8
C16	HC	26.4 ± 2.5	195.3 ± 19.0	675.9 ± 75.9
	LC	19.7 ± 4.4	245.5 ± 24.0	482.0 ± 27.8
H24	HC	22.2 ± 5.5	102.6 ± 2.0	149.6 ± 69.2
	LC	10.9 ± 5.2	92.0 ± 8.5	50.4 ± 9.1
H82	HC	27.6 ± 1.4	184.6 ± 27.4	425.2 ± 17.5
	LC	13.5 ± 5.2	179.5 ± 12.3	525.6 ± 75.1
P103	HC	13.7 ± 0.9	N.D.	N.D.
	LC	19.7 ± 2.0	168.8 ± 11.1	312.4 ± 9.9

Data are shown ± standard deviation, which were obtained from at least three independent experiments. Ci, inorganic carbon; HC, high CO_2; LC, low CO_2; N.D.; not determined; V_{max}, maximum O_2-evolving activity.
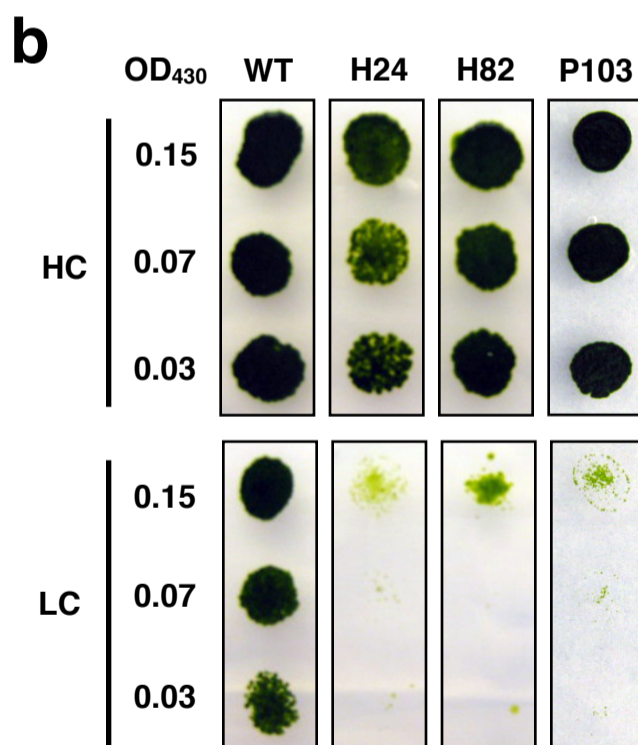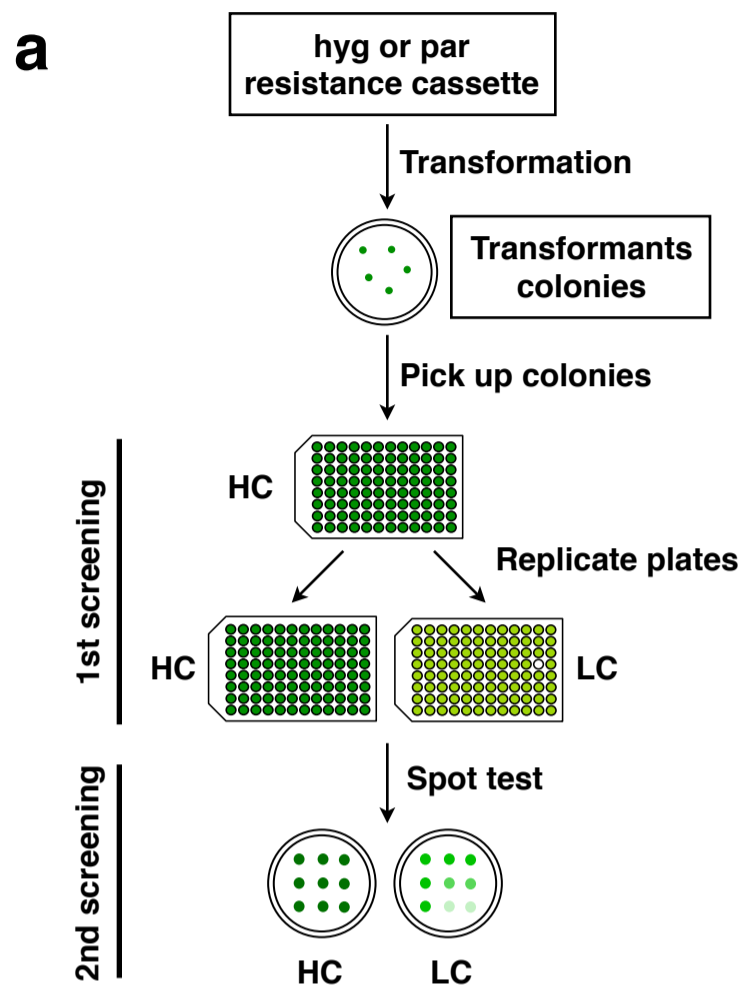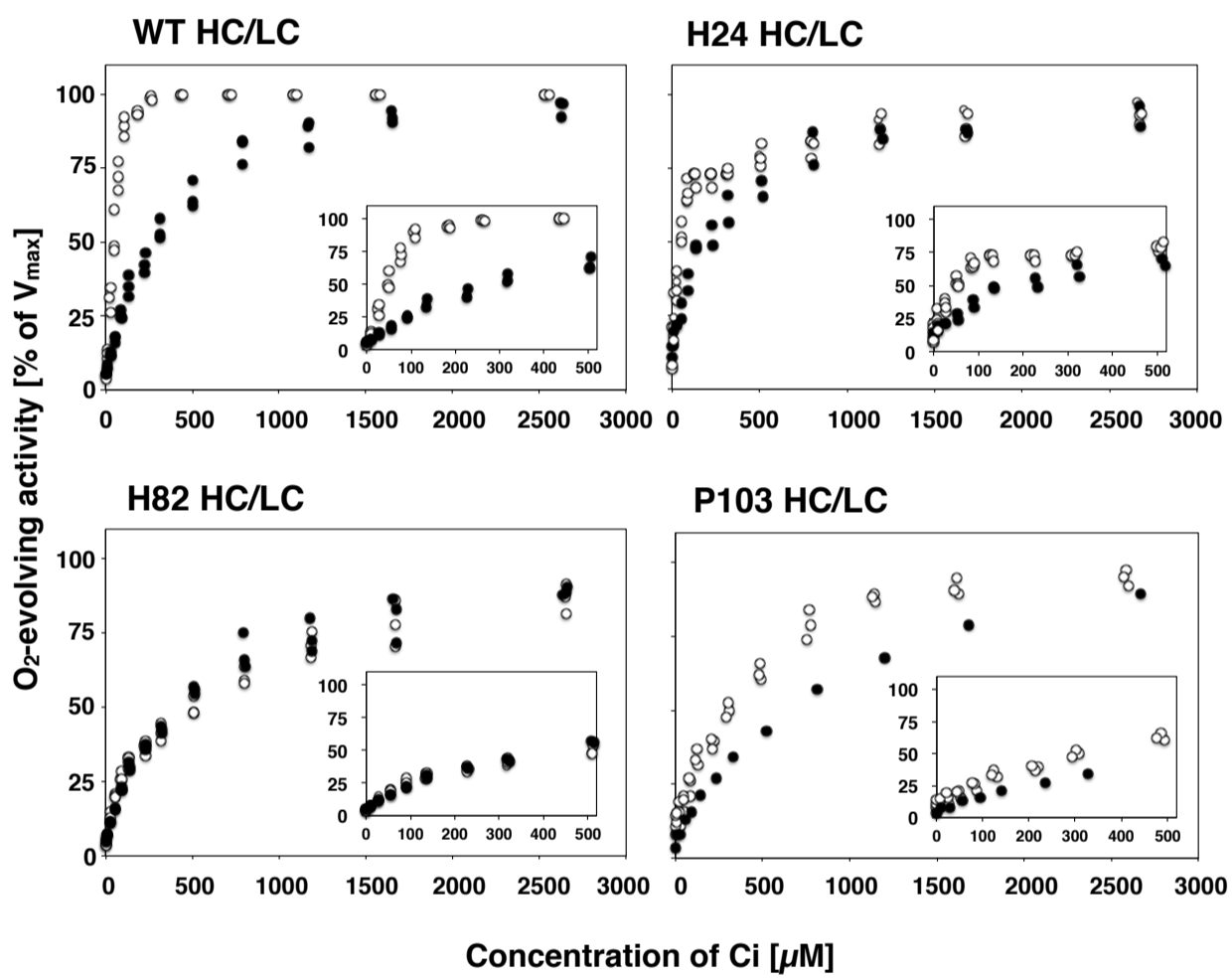
Figure 1

WT HC/LC

H24 HC/LC

H82 HC/LC

P103 HC/LC

O₂-evolving activity [% of V_max]

Concentration of Ci [μM]

Figure 2

Figure 3

a

H82 (mt⁻) × CC-1690 (mt⁺)

A1   A2   A3   A4

F1/UP-S

OD₄₃₀

0.15

0.07

0.03

b

Cre12.g497300 (*CAS*)

UP-S   DP-S

F1→   ←R1   ←R2

92 bp
deletion

c

WT   H82

M   F1/   F1/   F1/   F1/   M
     R1   UP-S   R1   UP-S

(bp)

8,000
6,000
4,000
3,000

2,000
1,650

1,000

600

400

300

d

HC   LC

WT   WT   H82   #10   #13

CAS-HA

*

LCIA

HLA3

e

Relative expression level

CAS
LCIA
HLA3

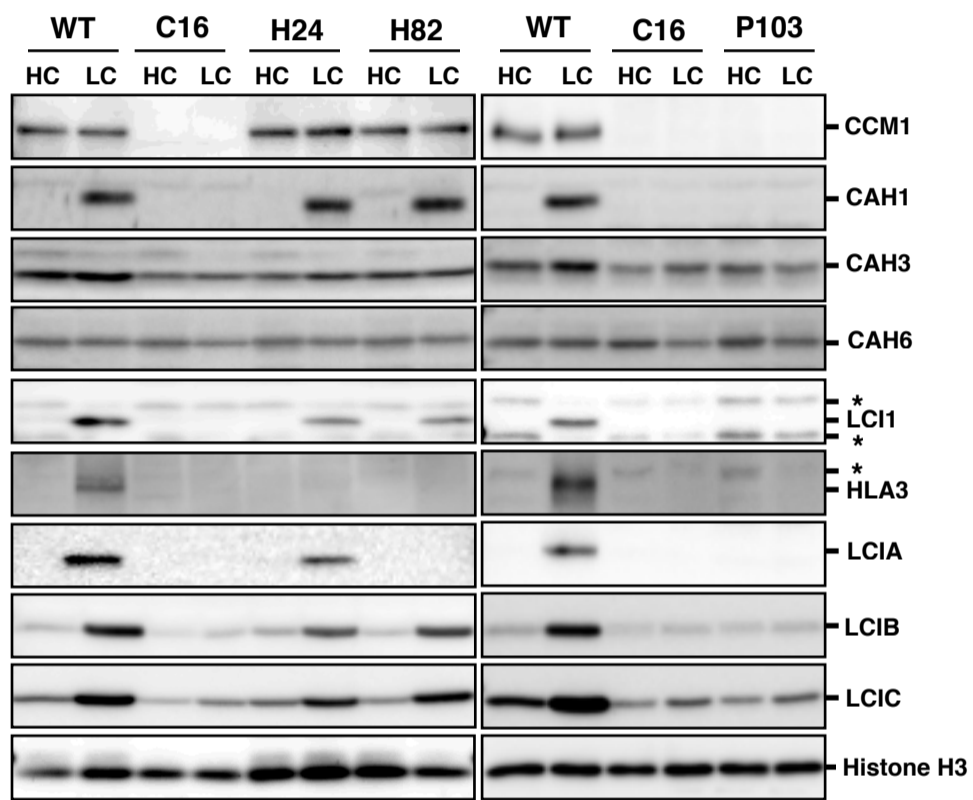HC LC   HC LC   HC LC   HC LC
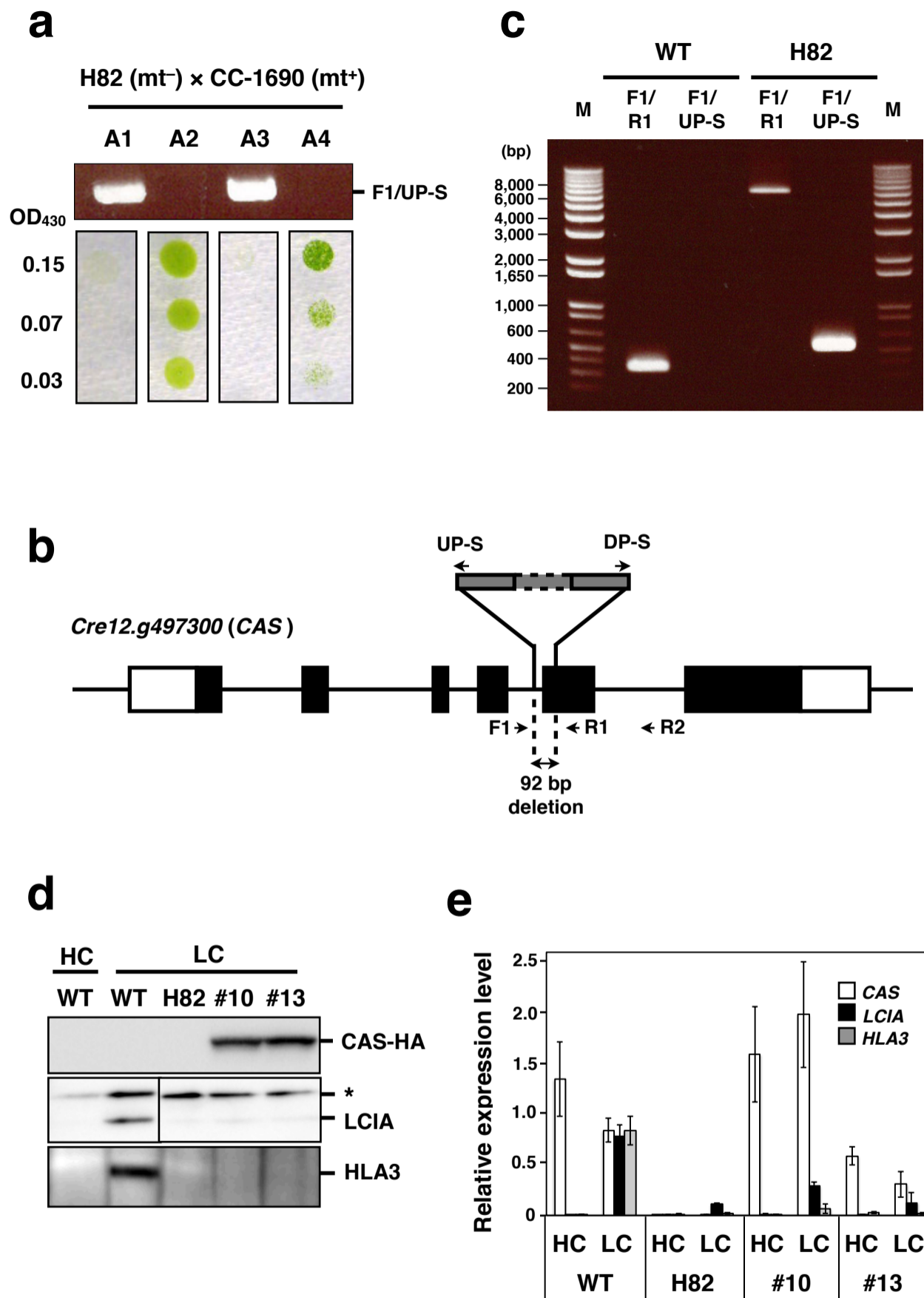
WT   H82   #10   #13

Figure 4

Supplementary material

Click here to download Supplementary material: Supplementary-figures.pdf